MICROSTRUCTURE AND SINTERING MECHANISM OF SiC CERAMICS REINFORCED WITH NANOSIZED ZrO_2

Eszter Bódis,[a]* Ádám Fábián,[a] Krisztián Bán,[b] Zoltán Károly, [a] Szilvia Klébert,[a] Anna Mária Keszler,[a] Péter Fazekas,[a] János Szépvölgyi[a]

Keywords: SiC, ZrO_2 nanofibres, mechanical properties, spark plasma sintering (SPS)

Silicon carbide-based (SiC) ceramics has attracted quite broad attention due to their excellent mechanical, chemical and thermal properties. However, their widespread industrial application is hindered by difficulties in sintering and poor fracture toughness of sintered bodies. In this work, we present an alternative way to produce SiC-based ceramics with improved microstructure and mechanical properties. We incorporated ZrO_2 nanofibres into the ceramic matrix to achieve a combined reinforcing effect of partially stabilized zirconia, namely fibre and phase transformation strengthening. For comparison, we also prepared silicon carbide ceramics containing yttria stabilized zirconia (YSZ) particles. SiC-based green bodies containing 5, 10 and 15 wt % ZrO_2 nanofibres and particles, respectively, were subjected to spark plasma sintering (SPS) at relatively low (1700 °C) temperatures with high heating and cooling rates. The effects of nanofibres on mechanical properties were studied by determining the Vickers hardness and Young's modulus of sintered ceramics from instrumented indentation tests. The microstructural patterns were investigated, as well.

*Corresponding Authors: Eszter Bódis
E-Mail: bodis.eszter@ttk.mta.hu
[a] Institute of Materials and Environmental Chemistry, Research Centre for Natural Sciences, Hungarian Academy of Sciences, Magyar tudósok krt 2., H-1117, Budapest, Hungary
[b] Department of Automobiles and Vehicle Manufacturing, Faculty of Transportation Engineering and Vehicle Engineering, University of Technology and Economics, Műegyetem rkp. 3, H-1111, Budapest, Hungary

Introduction

Silicon carbide-based (SiC) ceramics are considered as a high-performance engineering material because of their low density, high strength (~550 MPa) even at high temperatures, great hardness (~26 GPa), good oxidation resistance, high thermal conductivity (~120 W m^{-1} K^{-1}) and low thermal expansion coefficient ($4 \cdot 10^{-6}$ K^{-1}).[1] The covalent bonds among constituting atoms result in a very hard and strong material. Therefore SiC-based ceramics are being used in several applications even in extreme condition. However, due to the strong covalent bonds and the low self-diffusion coefficient SiC can be fully sintered only above 2000 °C. To have high density ceramics at lower temperature sintering aids, mainly oxides, are required.[2] Similarly to most ceramics, SiC is also brittle due to its low fracture toughness.[3] Thus, it is essential to incorporate certain reinforcing materials into the SiC matrix. Many studies focus on increasing the mechanical properties of SiC using different ceramic particles[4-5] or more recently carbon nanostructures, like carbon nanotubes (CNT), carbon fibres or graphene sheets.[6-8] However, carbon tends to be oxidized in air at elevated temperatures and it destroys the properties of such ceramics composites.[9] To avoid the degradation of reinforcing materials in air at elevated temperatures and to reach high thermal stability, application of oxide-type reinforcing material seems appropriate.

ZrO_2 ceramics have been widely utilized in harsh environments and load-bearing conditions due to their high fracture toughness (~9.3 $MPa \cdot m^{1/2}$), high melting point (2680 °C), excellent bending strength and good wear resistance. In many ceramic composites zirconia may enhance the fracture toughness by stress-induced, tetragonal (t) to monoclinic (m) phase transformation. Numerous papers have reported on increased mechanical properties of ceramics matrix composites due to incorporation of ZrO_2 particles.[10-12]

In our previous works[13] we reported that ZrO_2 nanofibres were even better reinforcing agents than ZrO_2 particles: addition of ZrO_2 nanofibres to Si_3N_4 matrix significantly improved the fracture resistance of composite as compared to Si_3N_4 monolith. It was explained by the simultaneous phase transformation and fibre toughening of ZrO_2 fibres.

Some papers in the literature have been focused on studying ZrO_2/SiC systems. However, in most cases ZrO_2 was the matrix material, which was reinforced by SiC particles or SiC fibres.[14-17] Addition of ZrO_2 nanofibres for reinforcing of SiC matrix has not been studied up to now.

In this work we investigated the effect of partially stabilized ZrO_2 nanofibres on the mechanical properties of SiC-based composite ceramics prepared by spark plasma sintering (SPS) at relatively low sintering temperature (1700 °C). For comparison, we studied the reinforcing effect of ZrO_2 particles, as well. The mechanical properties of composite ceramics were characterized in terms of Vickers hardness (HV) and Young's modulus. The phase composition and microstructure of sintered bodies were also studied in order to get some information on the mechanism of spark plasma sintering.

Methods

SiC-based ceramic composites were prepared by sintering commercial SiC powder (Washington Mills) containing ZrO_2 particles and nanofibres as reinforcing additives in concentration of 5, 10 and 15 wt %, respectively. A reference specimen was also prepared from SiC without reinforcement. Al_2O_3 powder (3 wt % of Alcoa, A16) was added as sintering aid to the green mixtures. Both commercial ZrO_2 particles (Sigma Aldrich, 99.0 %) and ZrO_2 nanofibres were partially stabilized by 3 mol % Y_2O_3. The nanofibres were prepared in our laboratory by electrospinning, as reported previously.[13]

The green mixtures, SiC matrices containing ZrO_2 fibres (SiC/ZrO_{2f}) or ZrO_2 particles (SiC/ZrO_{2p}) were prepared as follows: ZrO_2 nanofibres were dispersed in ethanol (Molar Chemicals, Hungary, 99.0 %) by ultrasonication for 30 min. The SiC and Al_2O_3 powders were mixed in a Fritsch planetary ball mill with alumina tank for 30 min at 400 rpm using alumina grinding balls (diameter: 10 mm). The SiC-Al_2O_3 powder blend and the ZrO_2 fibre dispersion were mixed with a magnetic stirrer for 30 min, followed by drying at 90 °C. Samples containing ZrO_2 particles and the reference sample (without ZrO_2) were prepared in the same way.

Discs prepared from the above green mixtures were subjected to spark plasma sintering (SPS) in a HD P5 sintering machine (FCT GmbH) at 1700 °C. The green bodies were heated in argon atmosphere (1 atm) at a rate of 200 °C·min^{-1} with on/off current pulses of 3/1 ms, at ~3500 A and ~5 V. Holding time of 4 min was applied at 1700 °C in each test. During sintering a uniaxial pressure of 50 MPa was applied. The sintered samples were cooled down to near room temperature at a rate of 150 °C·min^{-1}. The high heating and cooling rates were necessary to accelerate the sintering process and to avoid any inadvertent reactions. The heating current and voltage were recorded along with the shrinkage of green bodies.

The bulk densities of sintered ceramics were measured by the Archimedes' method, while their relative densities were calculated supposing theoretical densities of 3.2, 3.9 and 5.7 g·cm^{-3} for monolithic SiC, Al_2O_3 and ZrO_2, respectively.

The morphology and microstructure of the Pd coated composites were studied with a Zeiss EVO40 scanning electron microscope (SEM). The elemental composition and the distribution of the components were characterized by an Oxford INCA manufactured energy dispersive X-ray spectroscope (EDS).

The phase compositions of sintered samples were determined with a Philips PW 1830 X-ray diffractometer (XRD) in the 2θ range of 20-70°.

The Young's modulus and Vickers hardness were measured using an instrumented indention tester (CSM Instrument, 500 mN Vickers diamond indentation force for 15 s). The hardness and elastic modulus were calculated from the load-depth curves according to the Oliver and Pharr method.[18] The reported hardness and modulus values are the mean of at least 9 measurements.

Results and discussions

Relative densities

The relative densities of sintered SiC ceramics as above were plotted in Figure 1. The reference sample had a relative density of 89.7±0.2 %. A bit higher relative density of 91±0.1 % was obtained for SiC reinforced with 5 wt % ZrO_2 fibre. Further increase of ZrO_2 fibre content however, resulted in smaller relative densities. In the case of reinforcement with ZrO_2 particles an opposite trend was observed: the relative densities increased with the ZrO_2 content. The highest relative density of 90.7±0.1 % was observed for sample containing 15 wt % ZrO_2 particles. According to Kodash and co-workers,[19] the observed differences in the relative densities could be attributed to the high heating, because the intense current application hinders particles gliding, thus decreasing the rate of densification.

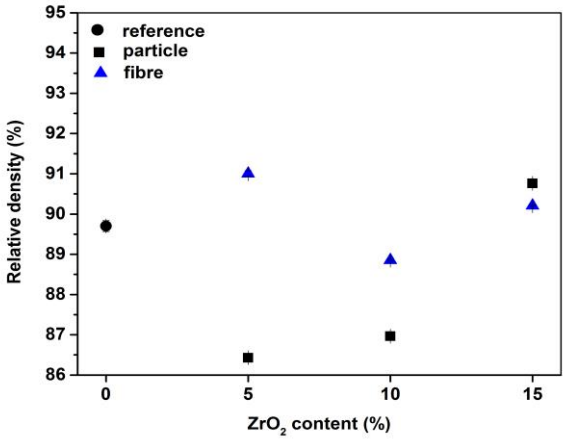

Figure 1. Relative densities of sintered SiC ceramics reinforced with ZrO_2 particles and fibres, respectively

Phase compositions

The XRD patterns of ZrO_2 fibres and commercial YSZ particles are shown in Figure 2. The ZrO_2 nanofibres consist of tetragonal (t) phase only, while the commercial ZrO_2 particles are composed of tetragonal and monoclinic (m) ZrO_2 phases in nearly equal amounts.

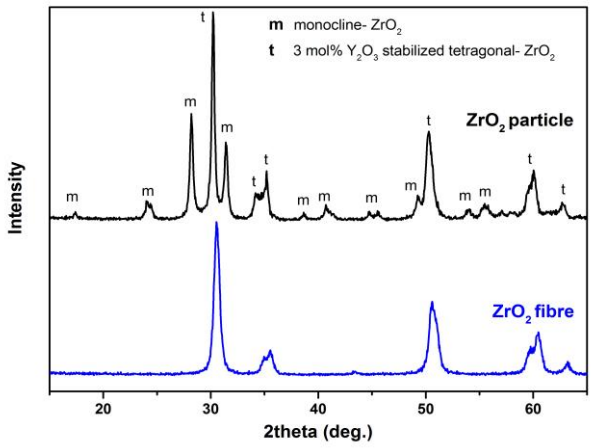

Figure 2. The XRD patterns of ZrO_2 nanofibres and particles

The diffraction patterns for both materials were in good agreement with the JCPDF2 card of the 3 mol % Y_2O_3 stabilized tetragonal ZrO_2 (JCPDF2 No. 83-113) and the card of the monoclinic ZrO_2 (JCPDF2 No. 13-0307), respectively. The XRD patterns of starting powder blends and sintered specimen of particular tests were shown in Figures 3a-b. In the starting powder blends the characteristic peaks of α-SiC crystallized in 6H-SiC and 4H-SiC polymorphs were detected.

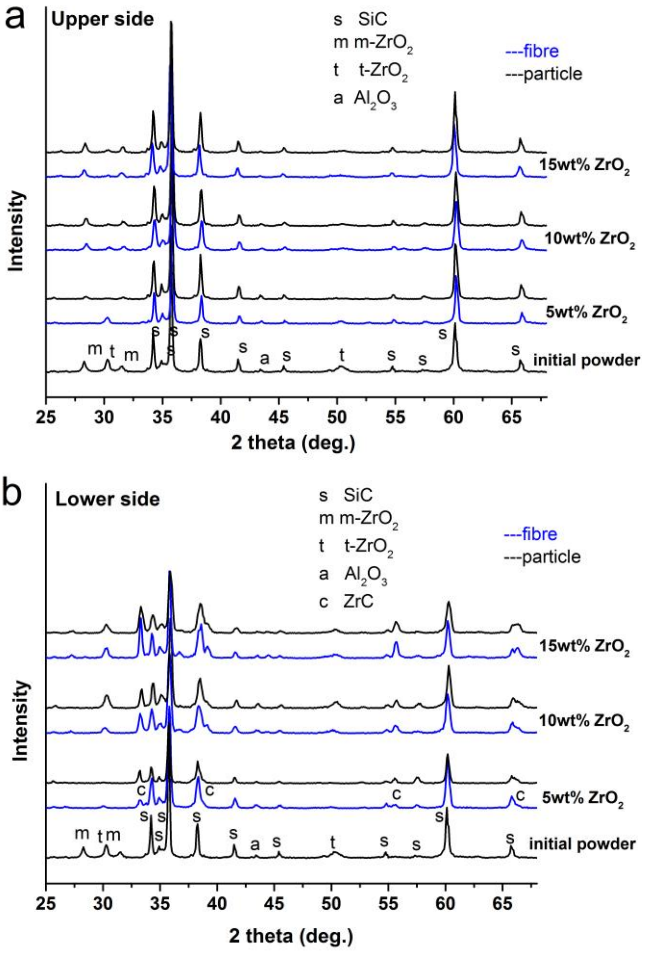

Figure 3. Phase composition of the starting powders blends initial powder and the sintered composites as detected by XRD: a)upper side, b) lower side

On the XRD patterns of sintered composites we observed an interesting phenomenon. ZrC was developed as a new phase due to a chemical reaction between SiC and ZrO_2 (Figure 3b). The newly-formed ZrC is highly crystalline with typical crystalline size of ~196 nm as determined by Scherrer equation. However, ZrC was detected only at the lower side of composite discs, while the other side of the discs (upper side) consists of ZrO_2 phases only in SiC matrix (Figure 3a). The SPS configuration is shown by the Figure 4, where the upper and bottom punches are marked. The amount of ZrC increased with increasing zirconia content, and it was a bit higher for the particle-reinforced composites than for the fibre-reinforced ones. We found further differences in the phase compositions on the opposite sides of sintered specimens. While the initial powders contained t-ZrO_2 and m-ZrO_2 in roughly equal amounts, after sintering the m-ZrO_2 phase practically disappeared, whilst the intensity of t-ZrO_2 increased on lower side. In contrast, on the upper side we could detect both phases of the ZrO_2, but the intensity of the t-ZrO_2 was significantly less comparing to the starting materials. The m-ZrO_2 → t-ZrO_2 transformation above 1170 °C is a well-known process that explains the tetragonal phase to be dominant on lower side. In case of fibre-reinforced composite, where only t-ZrO_2 phase was present, its amount did not change after sintering on lower side. On upper side m-ZrO_2 also appeared due to the t-ZrO_2 → m-ZrO_2 transformation. Lin et al.[20] supposed that alumina silicate glasses in the grain boundaries can scavenge yttrium ions from t-ZrO_2 grains, which is leading to a loss of stability of the tetragonal phase and t-ZrO_2 → m-ZrO_2 transformation can take place. In our case such transformation may also occur due to the presence of small glassy phase, even though we have not detected alumina silicate glass by XRD.

Differences in the phase compositions on the opposite sides of the sintered bodies can be attributed to the temperature differences between the different parts of graphite dies and by the different electrical conductivities of ZrO_2 and SiC. Anselmi-Tamburini et al. reported similar phenomenon in the case of cubic-ZrO_2 subjected to SPS for 5 min at 1200 °C under pressure of 105 MPa. However, they found just color differences between the two sides of the sintered bodies, because of the radial and axial temperature gradient during sintering and they suppose that the color gradient is a consequence of gradient in stoichiometry.[21]

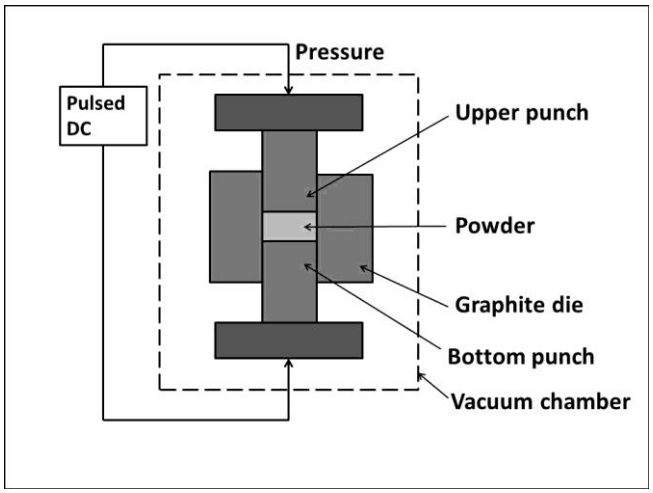

Figure 4. SPS configuration showing the graphite dies and punches

Microstructure

Figures 5a-b show the SEM micrographs of the initial powder blends. The size of SiC particles was around 3 μm, while the ZrO_2 particles were much finer with a mean size of ~0.8 μm (Figure 5b). The average diameter of ZrO_2 fibres as produced was ~0.5 μm; after ultrasonic treatment the length of the ZrO_2 fibres was ~5 μm (Figure 5a).

SEM micrographs of the fracture surface of sintered composites (Figures 6-8) show that grain growth of SiC can be minimized by the combination of short holding time and high heating rate (Figure 6). Both zirconia particles and fibres are evenly distributed in the ceramic matrix.

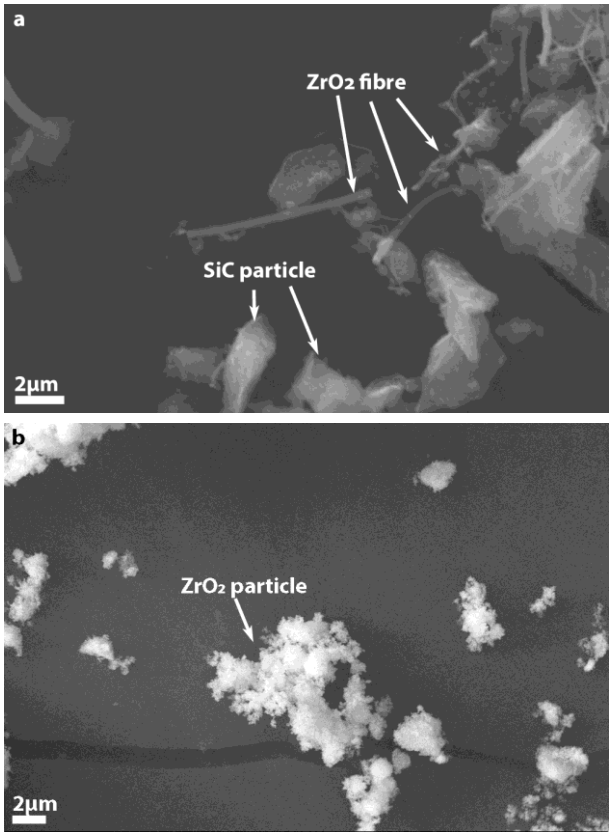

Figure 5. SEM micrographs of the initial SiC-Al_2O_3 powder mixtures with ZrO_2 nanofibres (a) ZrO_2 particles (b)

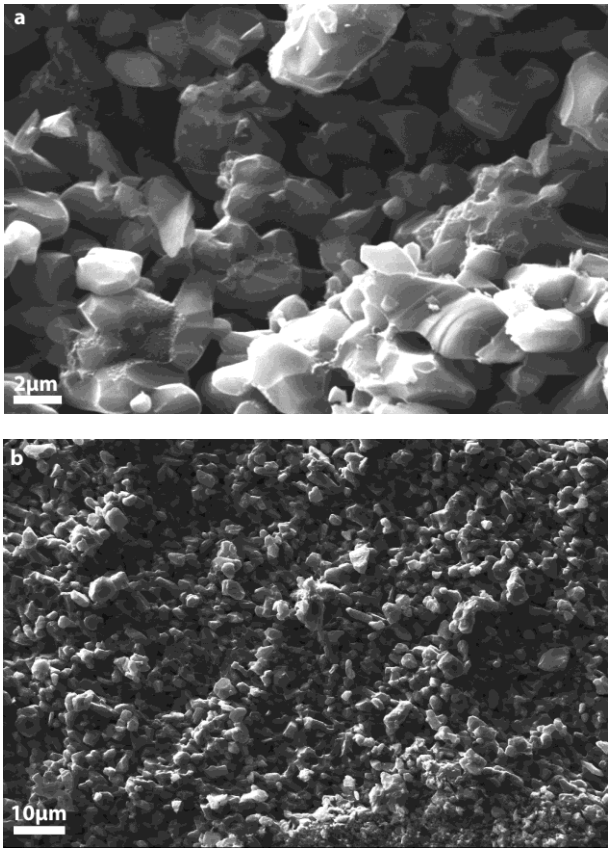

Figure 6. The fracture surface of the sintered reference SiC (secondary electron images)

In the case of fibre reinforcement, the zirconia fibres were well oriented due to uniaxial pressure during sintering. No orientation was detected in the particle-reinforced composite. SEM micrographs also revealed that the zirconia fibres did not preserve their original morphology on sintering; most ZrO_2 fibres and also the particles were melted during SPS, as it can be seen in Figures 7 and 8.

Zirconia has a melting temperature over 2500 °C, however, in contact with alumina being present as sintering aid, it could form an eutectic mixture having melting temperature much below 2000 °C.[22] As a consequence, in the fibre reinforced composite fibres could only be sparingly observed, while their original positions can be well detected by the dispersed traces.

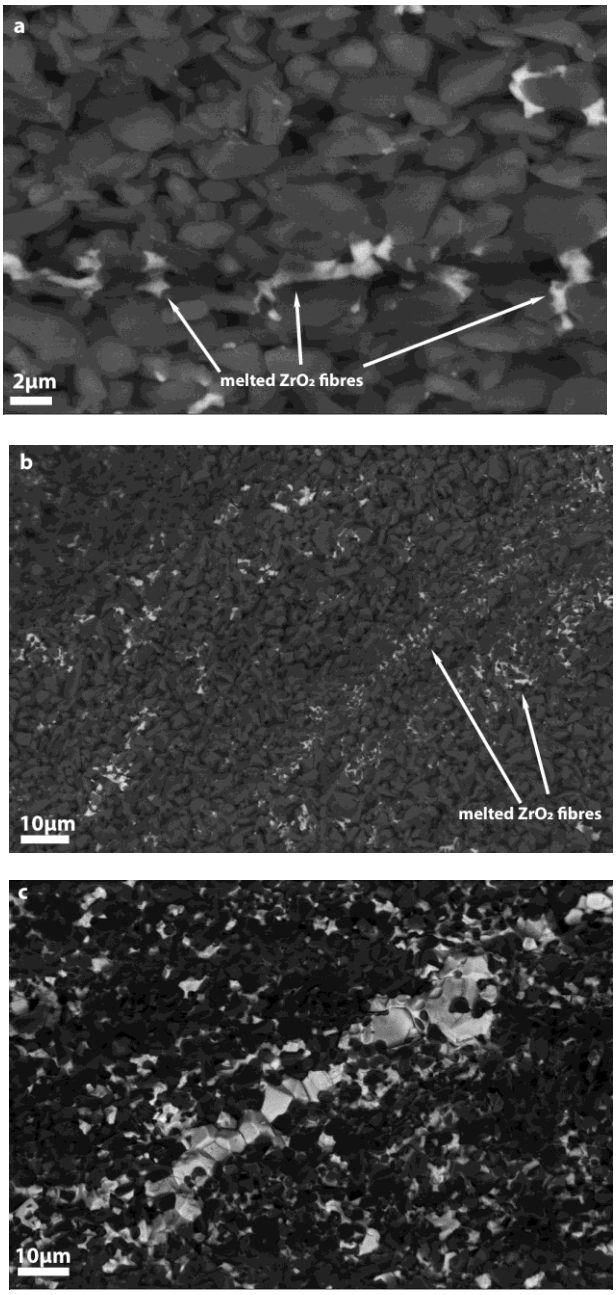

Figure 7. Fracture surfaces of sintered SiC reinforced with ZrO_2 nanofibres (backscattered electron images; (a, b) 10 wt% ZrO_2; (c) 15 wt% ZrO_2 nanofibres)

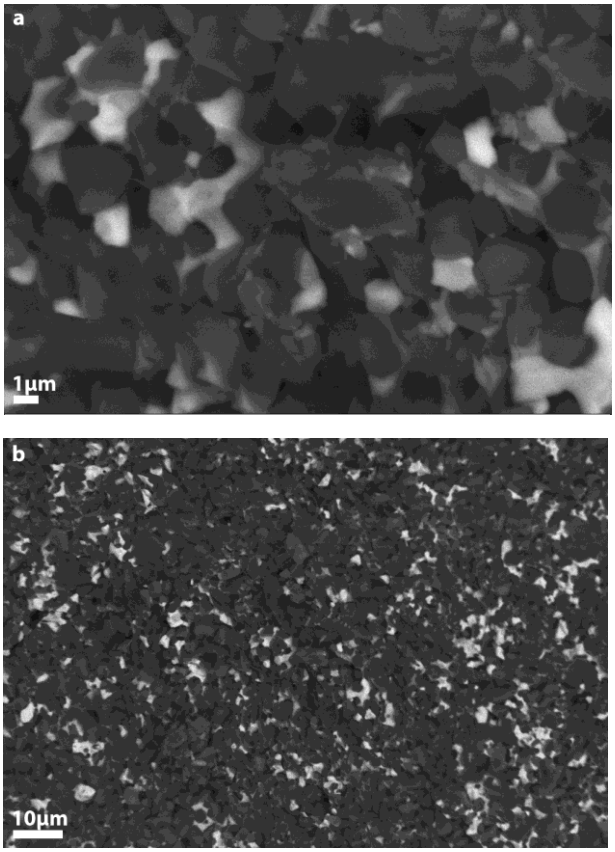

Figure 8. Fracture surface of sintered SiC matrix reinforced with 15 wt% ZrO_2 particle (backscattered electron images)

Energy dispersive X-ray spectroscopy (EDS) was also applied to get information about the microstructure and the newly formed ZrC in the SiC matrix containing 10 wt % ZrO_2 particles. Figure 9 shows the cross-sectional SEM micrographs and EDS mapping analysis of the two sides of specimen, while their composition was summarized in Table 1. Comparison of the concentrations of chemical elements on the two sides of specimen revealed that the concentration of C (27.73 at %) was higher on lower side than on the other (18.18 at %). However, on this side the concentrations of O and Si are less, than on the upper side, which confirmed formation of ZrC on lower side. The Pd came from the standard sample preparing procedure for SEM.

Table 1. Results of energy dispersive X-ray spectroscopy (EDS)

Element	Atomic%	
	Upper side	Lower side
C Kα	18.18	27.73
O Kα	17.35	13.31
Al Kα	1.80	1.95
Si Kα	55.62	50.42
Zr Kα	2.21	1.97
Pd Kα	4.83	4.62

At higher resolution, analysis of the element mapping showed the carbon distribution in the matrix (red dots in Figure 10). The carbon was detected at the grain boundary region of ZrO_2 particles. Based on this observation, we supposed that ZrC phase have been formed as an intergranular phase between ZrO_2 and SiC particles.

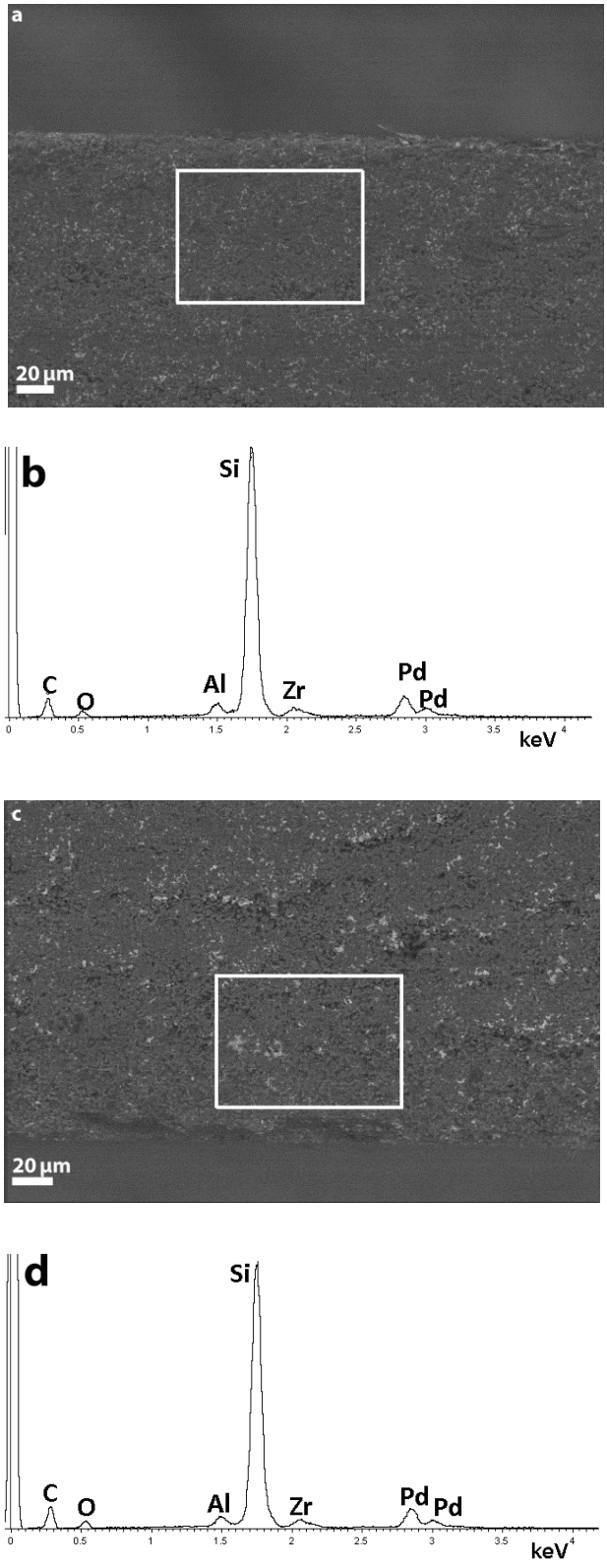

Figure 9. Results of EDS analysis of the sample containing 10 wt% ZrO_2 particles, a, c) morphology of the composites by SEM in cross- section view; b-d) results of EDS mapping

Mechanical properties

Because of the different phase compositions of the opposite surfaces of sintered specimens, as discussed above, we measured the mechanical properties on both sides of sintered composites.

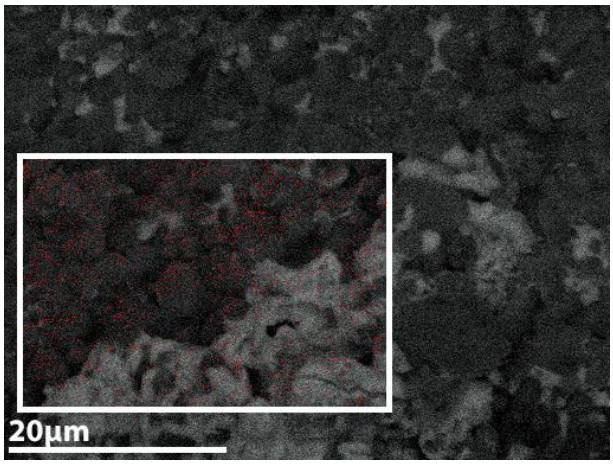

Figure 10. EDS element mapping analysis of the SiC/ZrO_{2p} fracture surface, showing the distribution of C element (red dots) in the matrix

Figure 11 clearly shows that incorporation of reinforcing additives into the SiC matrix significantly increased the hardness as compared to the reference specimen, regardless of the type of additive (particle or fibre). The improvement in hardness, however, depended both on the ZrO_2 content and the arrangement of samples during hardness measurements. On the ZrC containing lower side (dashed lines in Figure 11.) significantly higher Vickers hardness was measured regardless of the reinforcing material. The highest hardness (25.15±3.6 GPa) was measured for the specimen containing 5 wt % ZrO_2 particles. However, the hardness of particular composites decreased with increasing ZrO_2. In case of fibre containing composites quite similar tendency was observed, but the actual HV values were slightly lower than in particle cases. On the upper side (straight lines in Figure 11.) however, the SiC/ZrO_{2f} composites had higher HV values than the SiC/ZrO_{2p} ones.

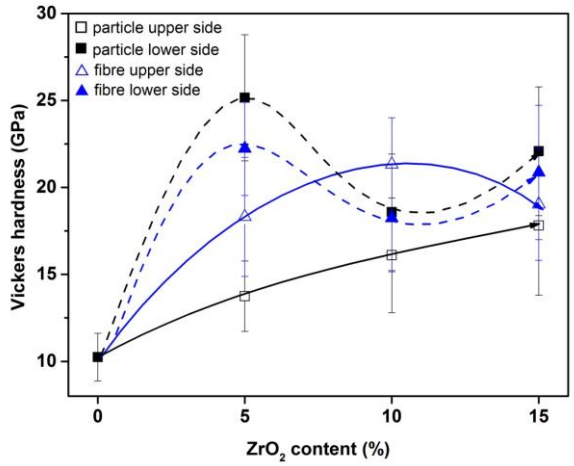

Figure 11. Vickers hardness of sintered SiC composites reinforced by ZrO_2 particles and fibres

Comparing with the other (lower) side, Vickers hardness exhibited a smaller, but continuous increase with zirconia content. The difference of HV values on the opposite sides of sintered samples can be attributed to the ZrO_2 + SiC → ZrC reaction.

In the particle containing composites more ZrC was formed that resulted in higher hardness on lower side as compared to the upper side.

Changes in the Young's modulus of specimens with zirconia content are similar to that in Vickers hardness. The reference specimen possessed the lowest modulus of 280.2±33.7 GPa. The elastic modulus tends to be significantly higher on the lower side than on the opposite side, due to presence of ZrC on this side of composite discs. Specimens containing ZrO_2 particles exhibit the highest modulus like the hardness. Adding ZrO_2 particles to the SiC matrix the modulus reached its maximum value (481.5±42.4 GPa) and a plateau at 10 wt % of ZrO_2 content. The modulus of the fibre containing composite was less by about a 100 GPa. On the upper side opposite tendency could be observed. The modulus increased with zirconia content both for fibre and particle reinforced composites. The SiC/ZrO_{2f} composite has a bit higher modulus than the SiC/ZrO_{2p} one, but they do not differ from each other on the upper side of composite discs. Comparing with the reference specimen a total improvement of 22.7 % was achieved in the modulus with a value of 345.08±19.2 GPa at 10 wt % ZrO_2 fibre content.

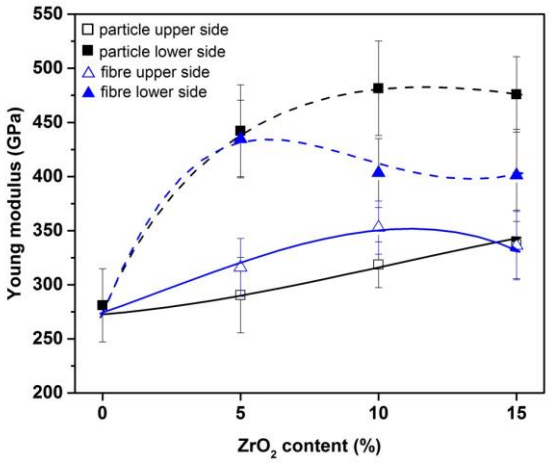

Figure 12. The Young's modulus for sintered SiC ceramics reinforced by ZrO_2 particles and fibres: dashed lines stand for upper side, while straight lines do for lower side

Conclusions

We produced silicon carbide-alumina (3 wt %) based composites containing partially (3 mol% Y_2O_3) stabilized ZrO_2 nanofibres and particles as reinforcing phases in concentrations of 5, 10 and 15 wt%, respectively, by spark plasma sintering. The 5 % SiC/ZrO_{2p} composite had the maximum relative density of 91.02 %. The density decreased with the ZrO_2 content of composites. We suppose that it is due to the relatively low sintering temperature (1700 °C) and the high heating and cooling rates. Polymorphic phase transformations and structural changes were detected on sintering. A new phase, namely ZrC was formed during sintering. It could be attributed to a chemical reaction between SiC and ZrO_2. Nevertheless, ZrC could be detected only on the lower side of sintered discs, while their other side only ZrO_2 was found in the SiC matrix.

SEM micrographs revealed that the zirconia fibres did not retain their original morphology on sintering. It was the consequence of the melting of ZrO_2 fibres and particles during SPS. In spite of changes in the morphology of fibres, their original positions can be well detected by their dispersed traces. EDS element mapping analysis showed carbon distribution at the grain boundary region of ZrO_2 particles, thus, the ZrC likely formed as intergranular phase between ZrO_2 and SiC grains. The side of disc containing ZrC phase had significantly higher Vickers hardness regardless of the reinforcing material. The highest hardness (25.15±3.6 GPa) was detected on the lower side of composite discs reinforced with 5 wt% ZrO_2 particles. Both Young's modulus and Vickers hardness changed similarly with the zirconia content of sintered bodies. On that side of sintered discs where ZrC was found, significantly higher elastic modulus was detected as compared to their opposite side. Composites containing particles exhibited the highest modulus, with a highest value of 481.5 GPa in the case of sample containing 10 wt% ZrO_2 particles. In summary, SPS technique is currently a powerful research tool for developing a SiC/ ZrO_2 composites; however the protection of the ZrO_2 particle and fibre are necessary to avoid the degradation of the reinforcing materials.

References

[1]Saddow. S. E., Agarwal. A., Advances in Silicon carbide processing and applications, *Silicon carbide Overview*, Artech House, Inc. Boston, **2004**, 1-23, ISBN 1-58053-740-5

[2]Raju, K., Yoon, D.-H., Sintering additives for SiC based on the reactivity: A review. *Ceram. Int*. **2016**, *42*, 17947-17962 http://doi.org/10.1016/j.ceramint.2016.09.022

[3]Sedláka. R., Kovalcíková. A., Girman. V., Múdra. E., Rutkowski. P., Dubield. A., Dusza. J., Fracture characteristics of SiC/graphene platelet composites, *J. Eur. Ceram. Soc*., **2017**, *37*, 4307-4314 https://doi.org/10.1016/j.jeurceramsoc.2017.04.067

[4]Kovalcíková,, A. Dusza, J. Sajgalík, P., Thermal shock resistance and fracture toughness of liquid-phase-sintered SiC-based ceramics, *J. Eur. Ceram. Soc*., **2009,** *29*, 2387-2394 https://doi.org/10.1016/j.jeurceramsoc.2009.01.021

[5]Shinoda Y., Suzuki Y., Yoshida K., TEM analysis of nanocrystalline SiC ceramics sintered by SPS using Al_2O_3-TiO_2 additive, *J. Asian Ceram. Soc.*, **2013,** *1*, 267-27 https://doi.org/10.1016/j.jascer.2013.06.004

[6]Feng, W., Zhang, L. T., Liu, Y. S., Li, X. Q., Cheng, L. F., Zhou, S. L., Bai, H., The improvement in the mechanical and thermal properties of SiC/SiC composites by introducing CNTs into the PyC interface, *Mater. Sci. Eng. A*, **2015,** *637*, 123-129 https://doi.org/10.1016/j.msea.2015.04.006

[7]Porwal, H., Tatarko, P., Saggar, R., Grasso, S., Kumar Mani, M., Dlouhý, I., Dusza, J., Reece, M. J., Tribological properties of silica-graphene nano-platelet composites, *Ceram. Int.,* **2014,** *40*, 12067-12074 https://doi.org/10.1016/j.ceramint.2014.04.046

[8]Young, R. J., Kinloch, I. A., Gong, L., Novoselov, K. S., The mechanics of graphene nanocomposites: A review. *Compos. Sci. Technol.*, **2012**, *72*, 1459-1476 https://doi.org/10.1016/j.compscitech.2012.05.005

[9]Porwal, H., Grasso S., Reecelm M. J., Review of graphene-ceramic matrix composites, *Adv. Appl. Ceram.*, **2013** *112*, 443-454. http://dx.doi.org/10.1179/174367613X13764308970581

[10]Markys, G. G., Lewis, M. H., Microstructure and Fracture Toughness of Hot-Pressed Zirconia-Toughened Sialon, *J. Am. Ceram. Soc.*, **1993**, *76*, 1401-1408 http://dx.doi.org/10.1111/j.1151-2916.1993.tb03918.x

[11]Hayashi, K., Yamakawa, A., Room temperature strength and microstructure of Si_3N_4-Y_2O_3-ZrO_2-Al_2O_3 ceramics, *Mater. Sci. Eng.*, **1988,** *105-106*, 175-182 https://doi.org/10.1016/0025-5416(88)90494-6

[12]Dutta, S., Buzek, B., Microstructure, Strength, and Oxidation of a 10 wt % Zyttrite-Si_3N_4 Ceramic, *J. Am. Ceram. Soc*., **1984**, *61*, 89-92 454 http://dx.doi.org/10.1111/j.1151-2916.1984.tb09621.x

[13]Bódis, E., Molnár, K., Mucsi, A., Károly, Z., Móczó, J., Klébert, Sz., Keszler, A. M., Fazekas, P., Szépvölgyi, J., Silicon nitride-based composites reinforced with zirconia nanofibres, *Ceram. Int.,* **2017,** *43*, 16811–16818 https://doi.org/10.1016/j.ceramint.2017.09.078

[14]Baklanova, N. I., Matvienko, A. A., Titov, A. T., The Effect of ZrO_2 Interphase on Interfacial Frictional Stresses in SiC/ZrO_2/SiC_f Composites, *Compos. Interfaces*, **2010,** *17*, 383–393 https://doi.org/10.1016/j.surfcoat.2010.10.025

[15]Petrovic, J. J., Bhattacharya, A. K., Honnell, R. E., Mitchell, T. E., ZrO_2 and ZrO_2-SiC particle reinforced $MoSi_2$ matrix composites, *Mater Sci. Eng. A*, **1992**, *155*, 259-266, https://doi.org/10.1016/0921-5093(92)90332-U

[16]Liu, D., Gao, Y., Liu, J., Li, K., Liu, F., Wang, Y., An, L., SiC whisker reinforced ZrO_2 composites prepared by flash-sintering, *J. Eur. Ceram. Soc*., **2016,** *36*, 2051-2055 https://doi.org/10.1016/j.jeurceramsoc.2016.02.014

[17]Padmavathi, N., Ghosal, P., Ray, K. K., Solution based processing and properties of carbon fiber reinforced SiC + ZrO_2 composites, *Compos. Sci. Tech*., **2015,** *106*, 55–59 http://dx.doi.org/10.1016/j.compscitech.2014.11.001

[18]Oliver, W. C., Pharr, G. M., An improved technique for determining hardness and elastic modulus using load and displacement sensing indentation experiments, *Mater. Res*., **1992**, *7*, 1564-1583 https://doi.org/10.1557/JMR.1992.1564

[19]Kodash V.Y., Groza J. R., Cho K. C., Klotz B. R., Dowding R. J., Field-assisted sintering of Ni nanopowders, *Mater. Sci. Eng*. A, **2004**, *385*, 367-371 https://doi.org/10.1016/j.msea.2004.06.075

[20]Lin, Y-J., Angelini, P., Mecartney, M. L., Microstructural and chemical influences of silicate grain-boundary phases in yttria-stabilized zirconia, *J. Amer .Ceram. Soc*., **1990**, *73*, 2728-35 https://doi.org/10.1111/j.1151 2916.1990.tb06753.x

[21]Anselmi-Tamburini U., Gennari S., Garay J. E., Munir Z. A., Fundamental investigations on the spark plasma sintering/synthesis process II. Modeling of current and temperature distributions, *Mater. Sci. Eng. A*, **2005**, *394*, 139-148 https://doi.org/10.1016/j.msea.2004.11.019

[22]Lakiza, S. N., Lopato, L. M., Stable and metastable phase relations in the system alumina-zirconia-yttria, *J. Am. Ceram. Soc.*, **1997,** *80*, 893-902 https://doi.org/10.1111/j.1151-2916.1997.tb02919.x

Received: 22.09.2017.
Accepted: 02.12.2017.